Second Conference on Smart Monitoring,
Assessment and Rehabilitation of Civil Structures

SMAR 2013

Finite element modeling for fatigue strengthening of metallic riveted bridges using un-bonded pre-stressed CFRP plates

G. Prinz[1], E. Ghafoori[2,3], A. Nussbaumer[1], M. Motavalli[2], A. Herwig[2], M. Fontana[3]

[1] EPFL, Swiss Federal Institute of Technology Lausanne, Steel Structure Laboratory (ICOM), Lausanne, Switzerland
[2] Empa, Swiss Federal Laboratories for Materials Science and Technology, Structural Engineering Research Laboratory, Dübendorf, Switzerland
[3] ETHZ, Swiss Federal Institute of Technology Zürich, Institute of Structural Engineering (IBK), Zürich, Switzerland

ABSTRACT: Many old riveted steel bridges remain operational and require retrofit to accommodate ever increasing demands. Complicating retrofit efforts, riveted steel bridges are often considered historical structures and as such structural modifications that affect the original construction are to be avoided. The presence of rivets along with preservation requirements often prevent the use of traditional retrofit methods, such as bonding of fiber reinforced composites, or the addition of supplementary steel elements. In this paper, an un-bonded post-tensioning retrofit method is numerically investigated using an existing riveted bridge geometry from Münchenstein, Switzerland. Pre-stressed un-bonded carbon fiber reinforced plastic (CFRP) plates will be considered for the strengthening elements. By using prestressed CFRP plates, a portion of the permanent loads (such as the dead-weight) will be transferred to the strengthening element. Fatigue critical regions of the bridge are identified, and the effects of the un-bonded post-tensioning method on strength and fatigue susceptibility are explored.

1 INTRODUCTION

Steel structures subjected to repeated loads will ultimately fail through a process of material fatigue, with the material fatigue-life (number of resisted repeated load cycles) being directly related to the repeated load value. Higher loads typically correspond with lower fatigue-life. Many old riveted bridges still in operation are subjected to ever increasing loads and require retrofit to extend the remaining fatigue-life.

Many commonly used retrofit methods are prohibited or difficult to install on riveted bridges. Due to historic preservation requirements, municipalities often prohibit alteration of riveted steel bridges, including welding or bolting of additional steel elements. Additionally, retrofits that require some form of bonding or gluing, such as attachment of fiber reinforced composites, are difficult due to the presence of protruding rivet heads. Retrofit systems that don't require alteration of the existing structure (drilling of holes, addition of welds, etc.) or bonding/gluing of external members, are desired.

An un-bonded post-tensioning system using carbon fiber reinforced polymer (CFRP) plates, currently under development at the Swiss Federal Laboratories for Materials Science and Technology (Empa), may provide increased strength and increased fatigue life to riveted bridges while accommodating preservation requirements, Ghafoori et al. (2012). In the un-bonded CFRP system, post-tensioned CRFP plates are attached to clamps, which are then attached to beams using only friction. Unlike bonded CFRP plates, rivet heads don't interfere with the un-bonded system due to eccentricities between the CFRP plate and beam attachment. Also, no permanent modifications, such as holes or welds are added to the existing structure. By attaching the CFRP system to the underside of a riveted bridge beam, initial compressive stresses could be introduced in the lower chord, thus reducing the applied stress range and fatigue damage during loading.

In this paper, the effect of the un-bonded CFRP post-tensioning retrofit system on the fatigue susceptibility of an existing bridge in Münchenstein, Switzerland, is explored. Analytical models are used to determine critical fatigue locations and to investigate the relative effects of the post-tensioning retrofit on these locations. The paper begins by describing the modeling methods for a global bridge model including: an overview of the bridge geometry and element types, materials and loading, and simulation of the CFRP post-tensioning retrofit. Following, fatigue analysis with and without the retrofit are presented, considering multiple CFRP pre-stress levels. Conclusions about the effects of the post-tensioning retrofit method on bridge fatigue performance are provided.

2 MODELING METHOD

2.1 Geometry, element type and boundary conditions

A global model simulating an entire bridge geometry is created to analyze the entire system response and help identify fatigue critical locations. The global model geometry is based on construction documents of an existing riveted railway bridge in Münchenstein, Switzerland. The bridge consists of two longitudinal trusses connected by various cross-beams and cross-bracings. The existing bridge supports are skewed at nearly 45 degrees, creating a singly symmetric geometry. Figure 1 shows the basic bridge geometry, having a width and individual truss-bay length of around 5m. Individual brace geometries for the first five bays are also presented in Figure 1 (note that only five bays are presented due to symmetry).

In the global bridge model, four-node linear shell elements model all geometries within the connection regions (potential critical locations. Outside the connection regions, beam elements are used to reduce computational expense.

Mesh size can affect the accuracy and computational expense of an analysis. Typically, smaller element size is associated with higher computational expense. In the global bridge model, connection regions, braces, and the entire longitudinal beams, have four-node linear shell elements at a general mesh size of 50mm. While 50mm is a somewhat large element size for modeling of a standard structural connection, in the context of an entire bridge with a span of over 45m, 50mm provides enough detail (ten elements in the beam web height) with moderate computational cost. ABAQUS (2006) is used for all analyses.

Global boundary conditions of the bridge model simulate the actual support condition of the constructed bridge. Construction documents indicate that the bridge is simply supported, with pin connections on one end and simple bearing rollers on the other (allowing longitudinal translation).

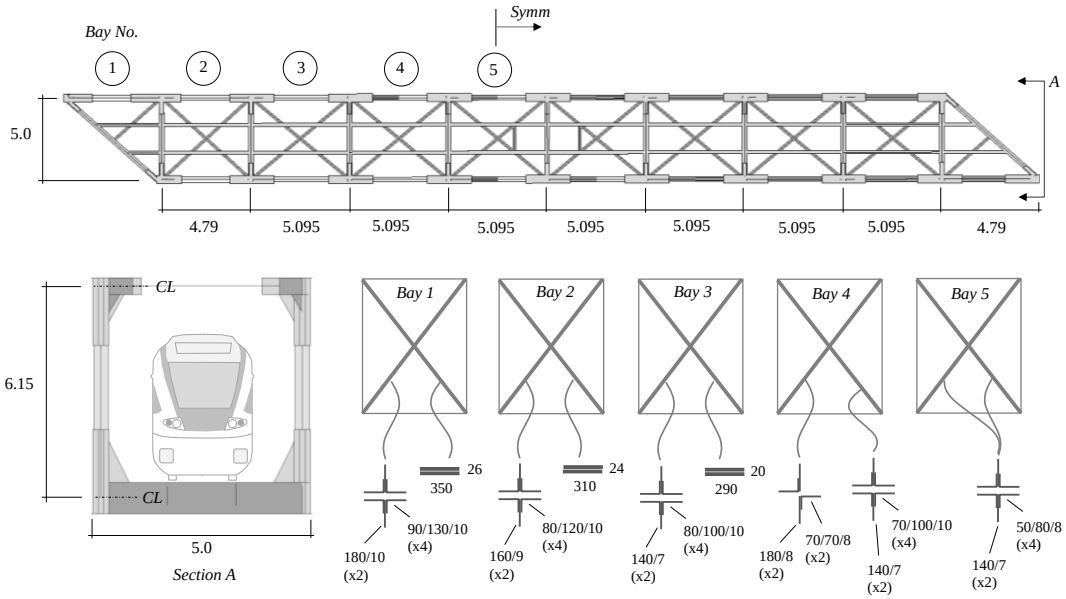

Figure 1. Münchenstein railway bridge basic geometry.

2.2 Material properties

Because only service loads are applied to the bridge, only elastic material properties are used in the analysis. Elastic properties for steel are relatively consistent between different steel grades (similar Young's modulus, E, and Poisson's ratio, ν). Typical steel values with an E of 210,000MPa and ν of 0.3 were considered in the analysis. An elastic stiffness of 165GPa and ultimate strength of 2,500MPa is assumed for the CFRP material.

2.3 Loading

Sequences of statically applied loads simulate passage of train axles along the bridge length. Vertical loads corresponding to individual axle weights are activated and deactivated in series, at different time steps, simulating a moving line load. Figure 2(a) shows the train axle loading scheme, with the different axle loads overlapping during the time steps. Since all loads are applied statically at each time-step, inertial effects and vibrations from previous axle passages are not included.

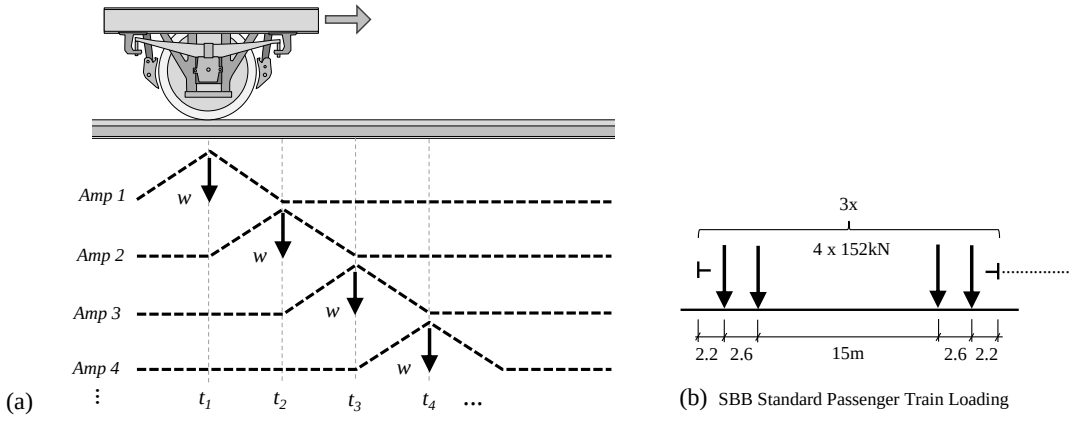

Figure 2. Train-axle loading scheme analysis.

To determine fatigue critical locations and to allow relative comparison between the retrofit and non-retrofit situations, a simple standard SBB (Swiss Federal Railways) passenger train (S01, including the locomotive) with individual axle weights equal to 152kN is considered, SBB (2002). Dynamic amplification factors are neglected as the loadings are simply used for relative performance comparisons. Figure 2(b) shows the axle spacing and weights for the SBB train load model. Note that only three passages of the SBB load model are considered in this study (three passages are required to fill the entire bridge length).

2.4 CFRP post-tensioning

Linear springs and connector elements simulate the CFRP post-tensioning system. Linear springs with applied pre-stress simulate the CFRP plate stiffness; and rigid connector elements provide the eccentricity between the CFRP plate and beam bottom flange (200mm assumed in this study). The spring pre-stress is applied by translating the material constitutive behavior, which normally has zero stress at zero displacement, until the desired pre-stress level occurs at zero displacement. Only one CFRP plate with dimensions of 50mm x 1.2mm is considered for strengthening of each cross-beam.

3 FATIGUE ANALYSIS COMPARISION

3.1 Critical regions and stress ranges on existing structure

To determine the bridge locations critical for fatigue, stress cycles from different locations are determined and compared. Figure 3 shows the stress range values resulting in the cross-beam web near the longitudinal-to-cross-beam connections. Figure 4 shows the stress range values resulting at the mid-span of the cross-beam bottom flange. Note in Figure 4, that the cross-beams near the supports are subjected to out-of-plane bending resulting from deformation of the longitudinal beams (deformation induced stresses). Fatigue damage resulting from these different stress range values (comparison of the stress ranges in Figure 3 and Figure 4) is determined through cycle counting and linear fatigue damage accumulation models (Miner's rule for example). Comparisons between the locations are made to determine effective positioning of the CFRP retrofit system.

Rainflow cycle counting and Miner's damage accumulation rule are used in this study. Using Miner's rule (see Equation 1), damage is dependent on the fatigue capacity at each applied stress range (see Equation 2), with higher stress range values leading to higher damage. Individual cycles, n_i, and stress range values, $\Delta\sigma$, are determined though a rainflow cycle counting procedure.

$$\sum D_i = \sum \left(n_i / N_i \right) \tag{1}$$

$$N_i = C\left(\Delta\sigma\right)^{-m} \tag{2}$$

In Equation 1, D_i, n_i, and N_i, are the damage, number of cycles, and number of cycles to failure, for each applied stress range, i. The number of cycles to failure in Equation 2 is based on the applied stress range ($\Delta\sigma$) and S-N curve parameters (C and m) where C represents the detail specific stress range failing at 2 million cycles ($\Delta\sigma_c^m$*2,000,000), Eurocode_3 (1993). Table 1 shows the resulting fatigue damage in the longitudinal-to-cross beam connection at each location, due to the standard SBB passenger train load model.

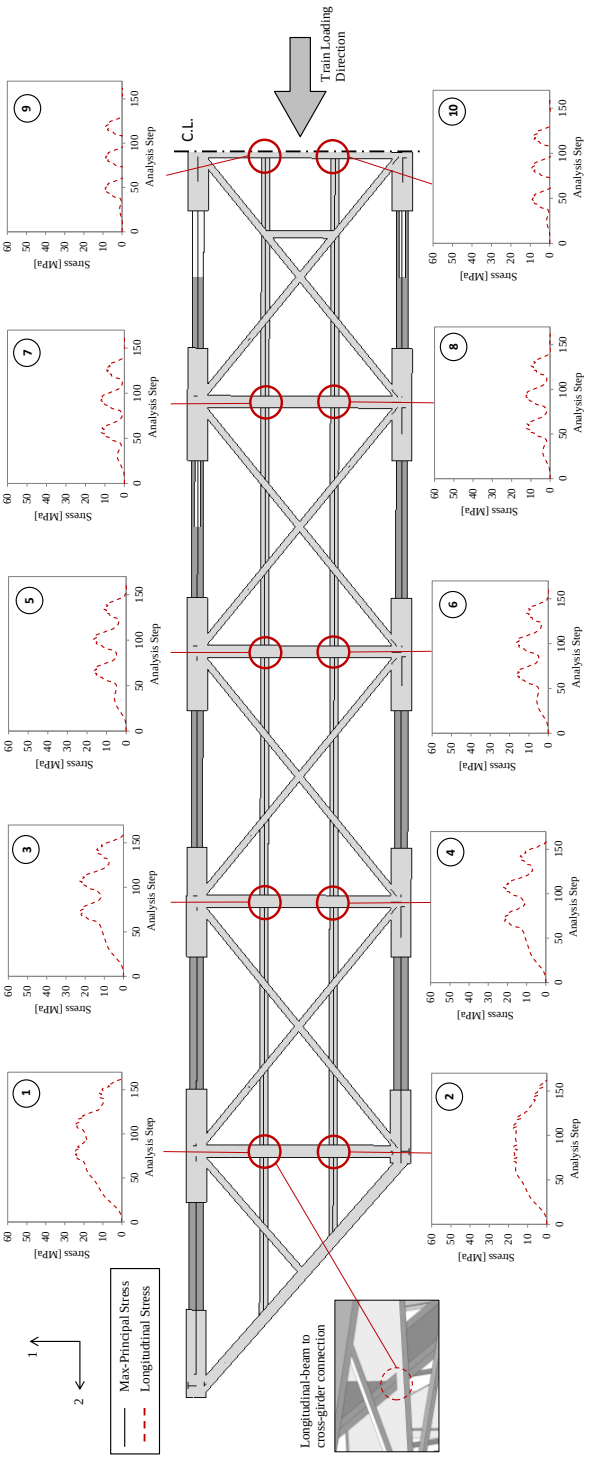

Figure 3. Longitudinal-to-cross girder stress ranges from SBB train load model (longitudinal stress, σ_{11}).

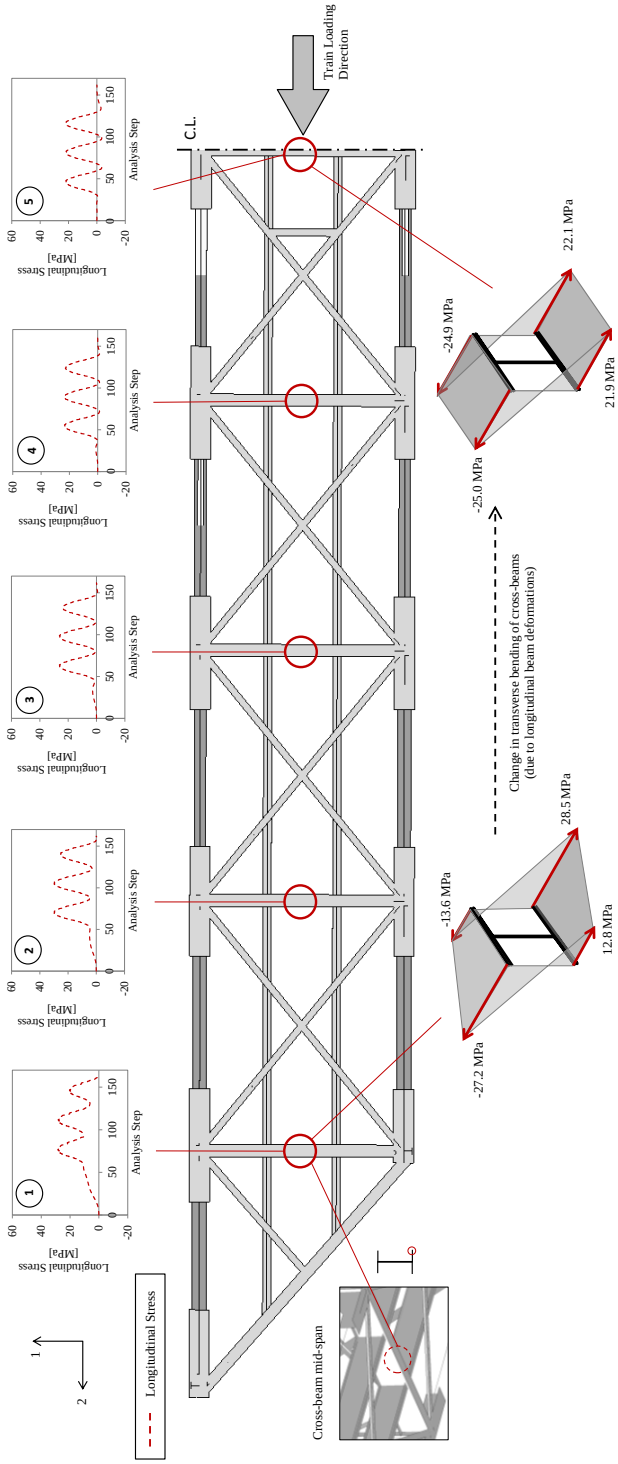

Figure 4. Cross-beam stress ranges at mid-span from SBB train load model (longitudinal stress, σ_{11}).

Table 1. Fatigue damage calculation for longitudinal-to-cross-beam connections

Location[a]	Stress Range [MPa]	Number of Cycles $[n_i]$	N_i[b]	Total Damage $[\Sigma D]$
1	24.30	1	4.99E+07	2.01E-08
	3.60	1	1.53E+10	
2	17.71	1	1.29E+08	7.76E-09
	--	--	--	
3	22.87	1	5.98E+07	1.78E-08
	9.31	1	8.87E+08	
4	21.98	1	6.74E+07	1.53E-08
	6.94	1	2.14E+09	
5	16.82	1	1.50E+08	8.39E-09
	10.76	1	5.75E+08	
6	16.77	1	1.52E+08	7.58E-09
	8.93	1	1.01E+09	
7	11.97	3	4.17E+08	7.19E-09
	--	--	--	
8	12.51	3	3.66E+08	8.21E-09
	--	--	--	
9	10.25	3	6.65E+08	4.51E-09
	--	--	--	
10	10.65	3	5.93E+08	5.06E-09
	--	--	--	

a. See Figure 3
b. $C=7.16\text{x}10^{11}$ and m=3, assumed from typical S-N curve data of riveted structures with detail category 71, SIA (2011).

Table 2. Fatigue damage calculation for cross-beam bottom flange locations

Location[a]	Stress Range [MPa]	Number of Cycles $[n_i]$	N_i[b]	Total Damage $[\Sigma D]$
1	28.46	1	4.44E+07	2.48E-08
	13.26	1	4.39E+08	
2	29.80	1	3.87E+07	2.58E-08
	22.76	1	8.69E+07	
3	21.06	3	1.10E+08	2.74E-08
	--	--	--	
4	25.00	3	6.55E+07	4.58E-08
	--	--	--	
5	25.54	3	6.15E+07	4.88E-08
	--	--	--	

a. See Figure 4
b. $C=1.02\text{x}10^{12}$ and m=3, assumed from typical S-N curve data of riveted structures with detail category 80, SIA (2011).

Table 2 shows the resulting fatigue damage in each cross-beam bottom flange. In Table 1 and Table 2, the number of cycles at each stress range and assumed values for C and m are presented. From Table 1, the highest damage in the longitudinal-to-cross-beam connection occurs at location 1, in the cross-beam closest to the bridge end; however, it is difficult to install the CFRP retrofit at this location due to space limitations near the supports. The next highest damage in the longitudinal-to-cross-beam connection occurs is at location 3, in the second cross-beam from the supports. From Table 2, the highest damage in the cross-beam bottom flange occurs at location 5, at the bridge mid-span. Comparing the two locations, it is determined that the cross-beam bottom flange is more critical (accumulating damage faster) than the longitudinal-to-cross-beam connection.

3.2 Effect of CFRP post-tensioning on fatigue susceptibility

Based on the global model fatigue results, the effects of the CFRP retrofit are investigated at two locations (the second cross-beam, location 3 in Figure 3, and the cross-beam at mid-span, location 5 in Figure 4). Four different levels of pre-stress (10, 20, 30, and 50%$\sigma_{u,CFRP}$) are considered at each location. Figure 5(a) and (b) show the resulting stress-range values at each critical location, for each level of CFRP pre-stress. From Figure 5, with increased CFRP pre-stress, a rigid shift in stress range history occurs, lowering the mean stress while the compressive-to-tensile stress ranges remain similar to the un-retrofitted case. Table 3 shows the resulting fatigue damage at each location and at each level of pre-stress.

With the non-welded details, a portion of the compressive stress ranges are neglected (40%) Eurocode_3 (1993), causing the rigid shift in mean stress to have a greater effect at the cross-beam bottom flange where each stress cycle dips into the compressive range. With an applied

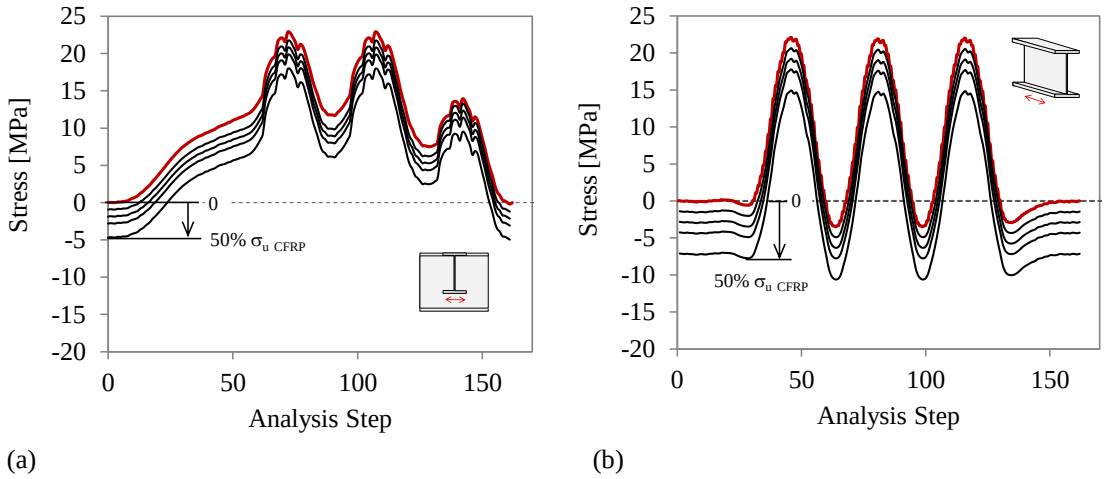

Figure 5. Critical stress range values at (a) longitudinal-to-cross beam connection and (b) cross-beam bottom flange for various CFRP pre-stress levels (0, 10, 20, 30, and 50%$\sigma_{u\ CFRP}$).

Table 3: Fatigue damage calculation at different CFRP pre-stress levels.

Location	CFRP Pre-Stress [%$\sigma_{u\ CFRP}$]	Mean Stress [MPa]	Stress Range [MPa]	Number of Cycles [n_i]	N_i	Total Damage [ΣD]	Fatigue Damage Reduction[e]
3[a]	10	9.79	22.16	1	6.58E+07[(c)]	1.73E-08	3.3%
			11.37	1	4.87E+08		
3	20	8.85	21.45	1	7.25E+07	1.58E-08	11.3%
			11.34	1	4.91E+08		
3	30	7.92	20.794	1	7.96E+07	1.43E-08	19.9%
			10.74	1	5.78E+08		
3	50	6.04	19.39	1	9.82E+07	1.15E-08	35.6%
			9.78	1	7.65E+08		
5[b]	10	4.67	22.65	3	8.81E+07[(d)]	3.48E-08	30.3%
5	20	3.24	22.39	3	9.12E+07	3.29E-08	32.6%
5	30	1.82	21.96	3	9.67E+07	3.10E-08	36.4%
5	50	-1.04	19.97	3	1.29E+08	2.33E-08	52.2%

[a.] See Figure 3
[b.] See Figure 4
[c.] C=7.16x10^{11} and m=3, assumed from typical S-N curve data of riveted structures with detail category 71, SIA (2011).
[d.] C=1.02x10^{12} and m=3, assumed from typical S-N curve data of riveted structures with detail category 80, SIA (2011).
[e.] Damage reduction from non-retrofitted case.

50%σ_u CFRP pre-stress, 35.6% and 52.2% reductions in fatigue damage are calculated at the longitudinal-to-cross beam connection and cross-beam bottom flange respectively. At lower pre-stress levels (10% σ_u) the damage reduction is much lower for the longitudinal-to-cross beam connection when compared to the cross-beam bottom flange (3.3% reduction versus 30.3% reduction). The CFRP retrofit has lower influence over fatigue at the longitudinal-to-cross beam connection due to the influence of the deformation induced stresses from the longitudinal bridge members, which are not affected by the cross-beam CFRP retrofit.

4 SUMMARY AND CONCLUSIONS

The effectiveness of an un-bonded pre-stressed CFRP retrofit on the fatigue susceptibility of an existing riveted bridge in Münchenstein, Switzerland, was explored. Global analytical models

with refinements within the connection regions were used to identify fatigue critical locations, and to gain insight into the retrofit effects. Since the primary goal of the study was to identify the critical regions, three passes of a standard SBB passenger train were used to load the bridge. The following conclusions are based on the global bridge analyses:

1) The longitudinal-to-cross beam connection near the end supports and the cross-beam bottom flange at the bridge centerline were determined to be the fatigue critical locations, with the cross beam bottom flange being more critical.

2) As expected, increased amounts of CFRP pre-stress result in decreased fatigue damage at both bridge locations.

3) The CFRP retrofit has a lower effect on fatigue at the longitudinal-to-cross beam connection compared to the cross beam bottom flange (3.3% reduction versus 30.3% reduction at a $10\%\sigma_{u,CFRP}$ pre-stress level) due to deformation induced stresses from the longitudinal members.

5 ACKNOWLEDGEMENTS

This project has been mainly funded by Swiss Commission of Technology and Innovation (CTI). Financial and technological supports from S&P Clever Reinforcement Company AG and Swiss Federal Railways (SBB) are acknowledged.

6 REFERENCES

ABAQUS, HKS. 2006. *ABAQUS Standard Users manual, Version 6.4*. Hibbitt, Karlsson, and Sorensen, Inc.

Eurocode_3.1993. Design of steel structrues - Part 1-9: Fatigue. *European Standard EN 1993-1-9. European Committee for Standardization*, Brussels, Belgium.

Ghafoori, E, Motavalli, M, Botsis, J, Herwig, A, Galli, M. 2012. Fatigue strengthening of damaged metallic beams using prestressed unbonded and bonded CFRP plates. *International Journal of Fatigue*, 44: 303–315.

SBB. 2002. *Richtlinie fur die Beurteilung von genieteten Eisenbahnbrucken*. I-AM 08/02. Ersetzt W Bau GD 27/92 / Rev. 96, Switzerland.

SIA. 2011. SIA 269/3 - Existing structures: steel structures. *Swiss Society of Engineers and Architects (SIA)*. Zurich, Switzerland.